IEICE Electronics Express, Vol.17, No.1, 1–5

LETTER

Tunable balanced BPF with wide tuning range and high selectivity

Xian Wang[1a)], Dewei Zhang[1], Qing Liu[1], Dalong Lv[1], Yi Zhang[1], and Shuxing Wang[1]

Abstract A highly-selective tunable balanced bandpass filter (BPF) with wide tuning range of center frequency is presented. The balanced BPF is designed by using compact varactor-tuned parallel coupled-line resonators with the direct-feed structure. It can realize a wide tuning range with an almost constant fractional bandwidth (CFBW). Three differential-mode (DM) transmission zeros (TZs) close to the tunable passband are obtained by mixed electromagnetic coupling and frequency-variant source-load (S-L) coupling. Meanwhile, the three TZs can almost keep the same relative location of passband to achieve continuous high selectivity and good out-of-band rejection over the whole frequency-tuning range. For verification, a tunable 1.02–3.25 GHz balanced BPF with three self-adaptive TZs is designed, fabricated and measured. And experimental and simulated results are in good agreement.

Keywords: balanced BPF, direct feed, wide tuning range, high selectivity
Classification: Microwave and millimeter-wave devices, circuits, and modules

1. Introduction

Recently, there has been a great interest in balanced bandpass filters (BPFs) on account of high immunity to crosstalk and electromagnetic interference [1, 2, 3, 4, 5, 6, 7, 8, 9, 10, 11, 12]. Considering the tunability and reconfigurability of RF/microwave system [13, 14, 15], the microstrip line resonator has been extensively utilized to design tunable balanced BPFs due to its simple manufacture process and easy integration with active devices. Accordingly, great efforts have been paid on tunable microstrip balanced BPFs [16, 17, 18, 19, 20, 21, 22, 23, 24]. The tunable differential-mode (DM) center frequency, bandwidth and high common-mode (CM) suppression have been designed in tunable balanced filters. In [25], by controlling the feeding structure, a tunable balanced BPF with high common-mode suppression is proposed. In [26], novel step-impedance resonators terminated with varactors (SIRTVs) based on coupled feed is proposed to widen the tuning range (up to 76.3%), but the selectivity of passband is poor. In [27], a high-selectivity tunable balanced BPF is proposed. Source-load (S-L) coupling are introduced for realizing two adaptive transmissions (TZs) on both sides of the tunable passband. However, the tuning range of center frequency is only 34.6%. The tuning range and selectivity of passband are very important parameters for tunable balanced filter. However, so far there is no reported work that can achieve both high selectivity and wide tuning range of 80%.

In this letter, a tunable balanced BPF with wide frequency-tuning range and high selectivity is proposed. To obtain the wide realization range of the external quality (Q_e), the direct-feed structure is proposed in the designed tunable balanced BPF. Due to the mixed coupling and frequency-variant S-L coupling, three transmission zeros are produced to improve the selectivity and out-of-band rejection. Meanwhile, the filter can maintain the continuous high selectivity and out-of-band rejection over the whole tuning range because of the self-adaptivity of three TZs. In addition, CM suppression can be realized by a pair of resistors loaded at the center of parallel coupled-lines. To validate this idea, a highly-selectively tunable balanced BPF with wide frequency-tuning range is implemented. And experimental and simulated results are in good agreement.

2. Design and analysis

Fig. 1 shows the proposed tunable balanced BPF. It consists of a parallel coupled-line resonator and lumped components. The direct-feed structure is adopted by the presented filter. Varactors C_{V1} are utilized to tune the center frequency. C_{V2} attached to the input/output feedlines are to adjust external coupling. In order to introduce the S-L coupling path, varactors C_{V3} are loaded between input and output feedlines. Besides, a pair of resistors R_1 are loaded at the center of coupled-lines to suppress the CM signals. And capacitances C_{block} (and C_1) and resistors are applied as dc block and dc bias, respectively.

When DM excitation is applied to the designed tunable balanced BPF in Fig. 1a, the central plane A-A′ can be considered as a virtual short. The DM equivalent circuit is shown in Fig. 1b. The direct-feed structure is adopted by the filter for several reasons: On the one hand, the coupled-feed structure is adopted by the majority of tunable balanced BPF [16, 17, 18, 25, 26, 27]. The coupled-feed line coupled resonator BPF typically leads to the realization problem in the external quality factor (Q_e) because of the line space limitation between the coupled-feed line and the resonator, which has been demonstrated by [28]. However, Q_e is the key factor to ensure a wide tuning range of center frequency. On the other, the feed-line coupling gaps lead to the coupling loss and transmission loss [29]. Thus, the direct-feed structure is selected for designing the filter.

[1]Department of Electromagnetic Wave and Antenna Propagation, National Digital Switching System Engineering and Technological Research Center, Zhengzhou, Henan 450001, China
a) 18595823270@163.com

DOI: 10.1587/elex.16.20190682
Received November 8, 2019
Accepted November 21, 2019
Publicized December 13, 2019
Copyedited January 10, 2020

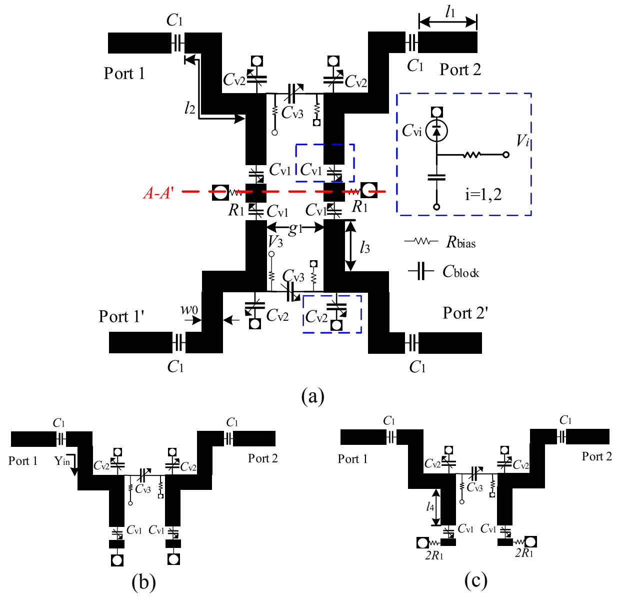

Fig. 1. (a) The structure of proposed balanced BPF. (b) DM equivalent circuit. (c) CM equivalent circuit

As indicated in DM equivalent circuit, varactor-tuned parallel coupled-line resonators are utilized to design the tunable balanced BPF. The resonant circuit contains coupled lines and C_{v1}. Thus, the input admittance Y_{in} is calculated,

$$Y_{\mathrm{in}} = jY_{\mathrm{L}} \frac{\omega_0 C_{\mathrm{V1}} + Y_{\mathrm{L}} \tan \beta_0 L}{Y_{\mathrm{L}} - \omega_0 C_{\mathrm{V1}} \tan \beta_0 L} \tag{1}$$

where β_0 represents the phase constant at resonant angular frequency ω_0, L is the physical length of resonator, $L = l_2 + l_3$. According to the resonance condition of $\mathrm{Im}[Y_{\mathrm{in}}] = 0$, and then the resonator frequency f_0 can be determined.

$$f_0 = -\frac{Y_{\mathrm{L}} \tan \beta_0 L}{2\pi C_{\mathrm{V1}}} \tag{2}$$

It can be found that f_0 is mainly determined by L and can be tuned by the varactor C_{v1}. When varactors are removed,

$$Y_{\mathrm{in}}{}' = jY_L \tan \beta_0 L = jY_L \tan \frac{2\pi f_0 L}{v_p} \tag{3}$$

where v_{p} is the phase velocity. According to the resonance condition of $\mathrm{Im}[Y_{\mathrm{in}}{}'] = 0$, the self-resonator frequency (f_0) can be calculated. The calculated and simulated results of self-resonant frequency with different values of L are shown in Fig. 2. As seen, both of them are in good agreement.

For keeping the CFBW, the desired coupling coefficient (M_{12}) and external quality factor (Q_{e}) should be constant across the whole frequency-tuning range. A BPF is initially designed with 0.043 dB ripple level and FBW of 8.5%. The desired theoretical value of M_{12} and Q_{e} can be calculated by [30]: $M_{12} = 0.14$; $Q_{\mathrm{e}} = 7.8$. Since the coupled-lines are placed in parallel, M_{12} mainly depends on the coupling gap (g_1) and length (l_3). Besides, the position of varactors C_{v1} can also influence the strength

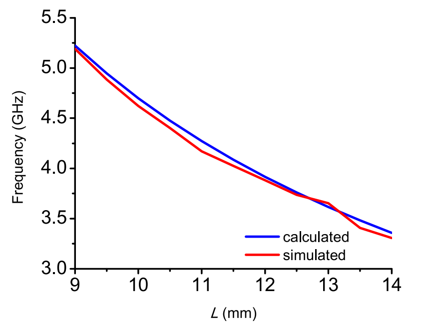

Fig. 2. Calculated and simulated self-resonant frequency with different values of L

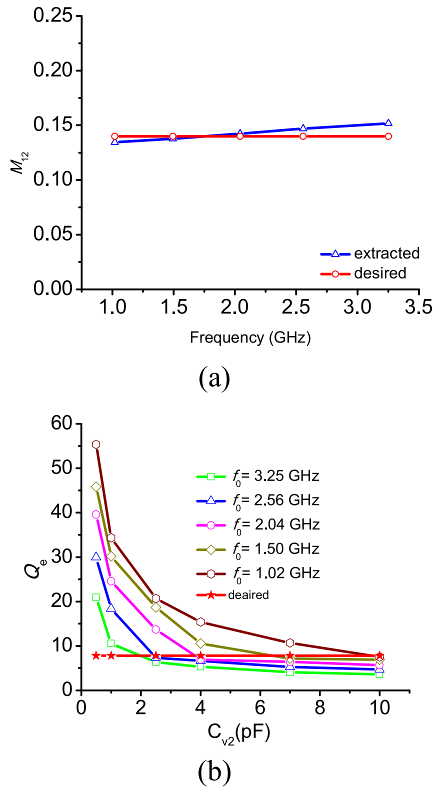

Fig. 3. Extracted and desired M_{12} and Q_{e}. (a) Extracted and desired M_{12} curves varied with center frequency. (b) Extracted and desired Q_{e} at different frequency versus C_{v2}.

of electric and magnetic coupling. So, it can provide another freedom to adjust M_{12}. The extracted M_{12} curves and desired M_{12} is shown in Fig. 3a. In order to control the external coupling, a pair of varactors C_{v2} are connected to the input and output feedlines. As shown in Fig. 3b, C_{v2} can tune the value of external coupling to the desired Q_{e} among the frequency-tuning process.

Fig. 4 shows the coupling topology of the DM equivalent circuit. Since the electromagnetic mixed coupling and frequency-variant S-L coupling are incorporated in this configuration, three TZs are produced.

Fig. 5 shows the limitation and effect of the varactor C_{v3} at 2.04 GHz. In the proposed parallel coupled line resonators, the magnetic coupling is adjusted by l_1 and g_0 and the electric coupling exists the open ends and corners of resonators. It is evident that the ratio of electric to

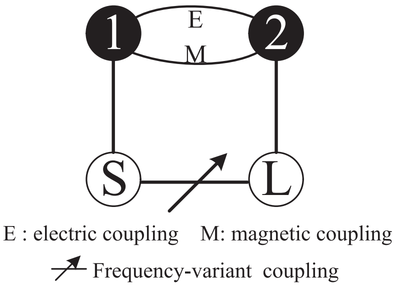

Fig. 4. The coupling topology of the DM equivalent circuit.

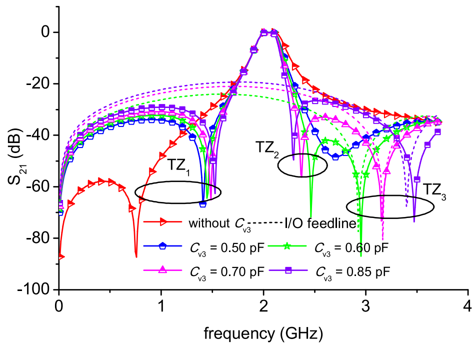

Fig. 5. The limitation and effect of the varactor C_{v3} at 2.04 GHz.

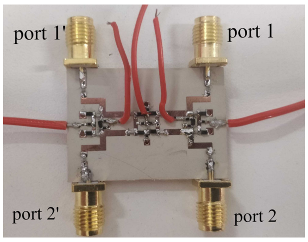

Fig. 6. The photograph of the fabricated tunable balanced BPF.

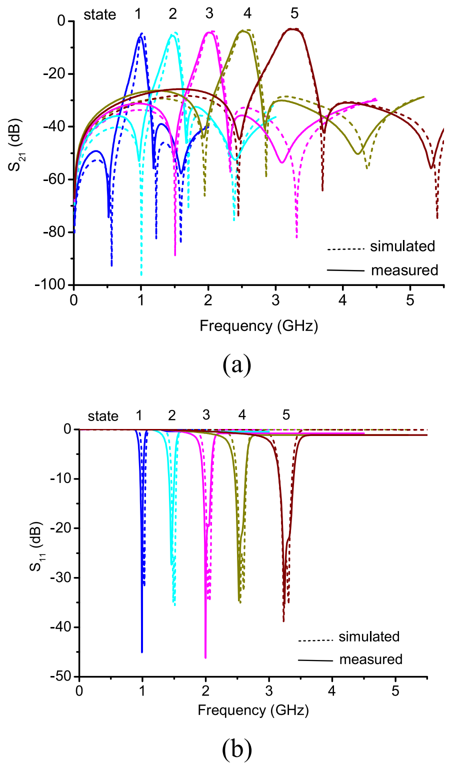

Fig. 7. Simulated and measured results of DM responses. (a) S_{21}. (b) S_{11}.

magnetic coupling coefficients E_C/M_C would be lower than 1. Form the formula $f_z/f_0 = \sqrt{E_C/M_C}$ in [31], f_0 is the center frequency, the TZ (TZ_1) is produced at the lower side of passband. When C_{v3} is added in I/O feedlines, two TZs (TZ_2 and TZ_3) are obtained. TZ_2 is generated due to the S-L coupling; TZ_3 is obtained for the characteristic of frequency-variant of the S-L coupling. To demonstrate the characteristic of frequency-variant, the resonators are removed from the structure and the I/O feedlines are simulated individually. As shown in Fig. 5 (dash line), TZ_3 can be still produced due to the frequency-variant coupling. TZ_1 and TZ_2 near the passband edges can be generated to enhance high selectivity; TZ_3 away from the passband is utilized to expand the out-of-band rejection.

For a high-performance tunable balanced BPF, high CM suppression in the wide frequency-tuning range is desirable. As CM excitation is applied to the designed filter in Fig. 1a, the central plane A-A′ can be treated as a virtual open. The CM equivalent circuit is shown in Fig. 1c. A pair of resistors R_1 are located at the center of parallel coupled-lines, which can decrease the CM unloaded quality factor Q_u of the resonator over the whole frequency-tuning range [5]. Therefore, a high CM suppression can be obtained in the DM operating frequency range.

3. Simulation and measured results

To verify the above discussion, the proposed tunable balanced BPF is designed and fabricated on the Rogers 3010 with a relative dielectric constant of 10.2, a thickness of 1.27 mm and a loss tangent of 0.0023. The optimized parameters of the designed filter are determined as follows: $w_0 = 1.21$ mm, $l_1 = 4$ mm, $l_2 = 7.71$ mm, $l_3 = 4.78$ mm, $l_4 = 1.2$ mm, $g_1 = 2.48$ mm $R_{bias} = 10\,\mathrm{K\Omega}$, $C_{\mathrm{block}} = 100$ pF, $C_1 = 4$ pF, $R_1 = 30\,\Omega$. Hyper abrupt junction tuning varactors SMV1281-097L and GaAs tuning varactor MA46H201 are adopted for $C_{V1(2)}$ and C_{V3}, respectively. The overall size of the filter is 32 mm × 22.5 mm or $0.35\,\lambda_g \times 0.24\,\lambda_g$, where λ_g represents the guided wavelength at at the lowest frequency passband (1.02 GHz). The photograph of the fabricated tunable filter is shown in Fig. 6. The simulation and measurement are conducted by ANSYS Electronics 18.0 and Network analyzer N5244A, respectively. Fig. 7 shows the simulated and measured results under DM excitation. As the voltage V_1 changes from 0–20 V, the operating frequency varies from 1.02–3.25 GHz, with tuning range of 104.4%. Meanwhile, the CFBW of 8.5 ± 0.5% can be obtained under the wide frequency-tuning range. Three self-adaptive TZs are introduced on both sides of the passband, ensuring continuous high selectivity and good out-of-band rejection (25 dB from 0 to 6.0 GHz). And the measured return loss and insertion loss across the entire tuning range are better than 22 dB and 5.1 dB, respectively. The CM responses are plotted in Fig. 8. As seen, over the DM operating frequency range, the CM suppression is better than 29 dB. Table I shows performance parameters and different control voltages/capacitances for five states listed. Table II is given to summarize the comparison of the proposed design with the previous tunable microstrip balanced BPFs. The proposed filter is highly competitive in terms of frequency-tuning range, DM selectivity and out-of-band rejection.

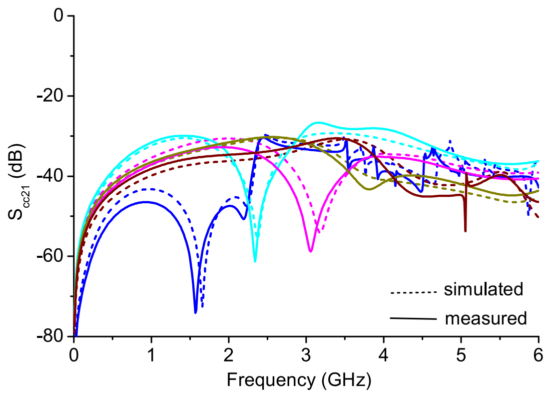

Fig. 8. The simulated and measured results of CM responses.

4. Conclusion

In this letter, a tunable balanced BPF with wide tuning range (up to 104.4%) and high selectivity is proposed. Due to the varactor-tuned parallel coupled-line resonators and the direct-feed structure, the CFBW and resonators and the direct-feed structure, the CFBW and wide tuning range of DM operating centre frequency is obtained. Three self-adaptive TZs are produced to enhance the selectivity and out-of-band rejection. Meanwhile, better than 29 dB CM suppression is obtained over the whole DM passband frequency-tuning range. Good agreements between the simulated and measured results demonstrate the validity of the proposed configuration, which has great potential in tunable and multi-purpose RF/microwave systems.

Table I. Performance parameters and different control voltages/capacitances for five states listed

state	f_0 (GHz)	FBW (%)	IL (dB)	S_{cc21} (dB)	V_1 (V)/C_{v1} (pF)	V_2 (V)/C_{v2} (pF)	V_3 (V)/C_{v3} (pF)
1	1.02	8.09	5.1	30.5	0/13.30	0.7/9.80	2.1/1.70
2	1.50	8.29	4.5	29.1	2.9/5.00	2.6/5.57	2.7/1.26
3	2.04	8.57	3.8	32.7	5.8/2.20	4.2/3.38	4.1/0.78
4	2.56	8.84	3.2	30.2	8.5/1.30	5.6/2.32	6.2/0.62
5	3.25	9.03	2.5	30.6	20.0/0.69	7.6/1.53	14.5/0.34

Table II. Comparison of the proposed design with the previous tunable microstrip balanced BPFs.

Ref.	FTR	BW	IL (dB)	TZs	Scc21 (dB)	Size (λ_g^2)
[16]	1.17–1.92 GHz (48.5%)	9.6 ± 0.35 (%)	2.9–6.0	2	>23	0.149
[25]	0.84–1.15 GHz (31.2%)	×	1.6–2.7	0	>50	0.015
[26]	0.73–1.63 GHz (76.3%)	9.8 ± 1.2 (%)	1.7–6.0	0	>43	0.063
[27]	1.60–2.27 GHz (34.6%)	137 ± 2 (MHz)	2.0–4.2	2	>30	0.136
This work	1.02–3.25 GHz (104.4%)	8.5 ± 0.5 (%)	2.5–5.1	3	>29	0.084

Note: FTR is the frequency-tuning range. BW is the bandwidth. IL is the insertion loss.

References

[1] J. Chen, *et al.*: "Analysis and design of balanced dielectric resonator bandpass filters," IEEE Trans. Microw. Theory Techn. **64** (2016) 1476 (DOI: 10.1109/TMTT.2016.2546260).

[2] Q.-Y. Lu, *et al.*: "A novel balanced bandpass filter based on twin-coaxial resonator," IEEE Microw. Wireless Compon. Lett. **27** (2017) 114 (DOI: 10.1109/LMWC.2016.2646906).

[3] K. Zhou, *et al.*: "Compact dual-band balanced bandpass filter based on double-layer SIW structure," Electron. Lett. **52** (2016) 1537 (DOI: 10.1049/el.2016.1968).

[4] Q. Lu, *et al.*: "A novel balanced bandpass filter based on twin-coaxial resonator," IEEE Microw. Wireless Compon. Lett. **27** (2017) 114 (DOI: 10.1109/LMWC.2016.2646906).

[5] A. Fernández-Prieto, *et al.*: "Simple and compact balanced bandpass filters based on magnetically coupled resonators," IEEE Trans. Microw. Theory Techn. **63** (2015) 1843 (DOI: 10.1109/TMTT.2015.2424229).

[6] P. Chu and K. Wu: "Balanced dual-mode SIW filter," Electron. Lett. **55** (2019) 208 (DOI: 10.1049/el.2018.7289).

[7] Q. Liu, *et al.*: "Balanced triple-mode substrate integrated waveguide bandpass filter," Electron. Lett. **55** (2019) 843 (DOI: 10.1049/el.2019.1731).

[8] S. Zhang, *et al.*: "Compact balanced bandpass filter with the fractal defected structures," IEICE Electron. Express **15** (2018) 20180518 (DOI: 10.1587/elex.15.20180518).

[9] B. Ren, *et al.*: "Balanced tri-band bandpass filter using sext-mode stepped-impedance square ring loaded resonators," IEICE Electron. Express **15** (2018) 20180670 (DOI: 10.1587/elex.15.20180670).

[10] J. Shi and Q. Xue: "Novel balanced dual-band bandpass filter using coupled stepped-impedance resonators," IEEE Microw. Wireless Compon. Lett. **20** (2010) 19 (DOI: 10.1109/LMWC.2009.2035954).

[11] P. Chu, *et al.*: "Balanced hybrid SIW–CPW bandpass filter," Electron. Lett. **53** (2017) 1653 (DOI: 10.1049/el.2017.3649).

[12] J. Shi and Q. Xue: "Balanced bandpass filters using center-loaded half-wavelength resonators," IEEE Trans. Microw. Theory Techn. **58** (2010) 970 (DOI: 10.1109/TMTT.2010.2042839).

[13] D. J. Simpson, *et al.*: "Single-/multi-band bandpass filters and duplexers with fully reconfigurable transfer-function characteristics," IEEE Trans. Microw. Theory Techn. **67** (2019) 1854 (DOI: 10.1109/TMTT.2019.2899849).

[14] Y. Ou and G. M. Rebeiz: "Lumped-element fully tunable bandstop filters for cognitive radio applications," IEEE Trans. Microw. Theory Techn. **59** (2011) 2461 (DOI: 10.1109/TMTT.2011.2160965).

[15] E. E. Djoumessi and K. Wu: "Tunable multi-band direct conversion receiver for cognitive radio systems," IEEE MTT-S International Microwave Symposium Digest (2009) 217 (DOI: 10.1109/MWSYM.2009.5165671).

[16] Y. Li and Q. Xue: "Tunable balanced bandpass filter with constant bandwidth and high common-mode suppression," IEEE Trans. Microw. Theory Techn. **59** (2011) 2452 (DOI: 10.1109/TMTT.2011.2161325).

[17] S. Zhang, *et al.*: "Compact tunable balanced bandpass filter with novel multi-mode resonator," IEEE Microw. Wireless Compon. Lett. **27** (2017) 43 (DOI: 10.1109/LMWC.2016.2629965).

[18] P. Chi and T. Yang: "Novel 1.5–1.9 GHz Tunable single-to-balanced bandpass filter with constant bandwidth," IEEE Microw. Wireless Compon. Lett. **26** (2016) 972 (DOI: 10.1109/LMWC.2016.2623251).

[19] D. Borah and T. S. Kalkur: "A balanced dual-band tunable bandpass filter," International Applied Computational Electromagnetics Society Symposium (ACES) (2018) 1 (DOI: 10.23919/ROPACES.2018.8364298).

[20] X. T. Zou, *et al.*: "Compact tunable balanced bandpass filter using a folded s-shaped slotline resonator (FSSR)," International Conference on Microwave and Millimeter Wave Technology (ICMMT) (2018) (DOI: 10.1109/ICMMT.2018.8563452).

[21] X. Zhu, *et al.*: "Novel reconfigurable single-to-balanced, power-dividing, and single-ended filter with frequency and bandwidth control," IEEE Trans. Microw. Theory Techn. **67** (2019) 670 (DOI: 10.1109/TMTT.2018.2882501).

[22] F. Wei, *et al.*: "Tunable balanced bandpass filter with high common-mode suppression based on SLSRs," Frequenz **71** (2017) 499 (DOI: 10.1515/freq-2016-0357).

[23] X. Zhu, *et al.*: "A tunable single-to-balanced bandpass filter with bandwidth control," Asia-Pacific Microwave Conference (APMC) (2018) (DOI: 10.23919/APMC.2018.8671678).

[24] Y. F. Pan, *et al.*: "A frequency tunable patch bandpass filter with wide tuning range," IEEE Asia-Pacific Conference on Antennas and Propagation (APCAP) (2018) 227 (DOI: 10.1109/APCAP.2018.8538054).

[25] X. Zhao, *et al.*: "Tunable balanced bandpass filter with high common-mode suppression," Electron. Lett. **51** (2015) 2021 (DOI: 10.1049/el.2015.1922).

[26] J. Mao, *et al.*: "Tunable differential-mode bandpass filters with wide tuning range and high common-mode suppression," IET Proc. Microw. Antennas Propag. **8** (2014) 437 (DOI: 10.1049/iet-map.2012.0203).

[27] W. Zhou and J. Chen: "High-selectivity tunable balanced bandpass filter with constant absolute bandwidth," IEEE Trans. Circuits Syst. II, Exp. Briefs **64** (2017) 917 (DOI: 10.1109/TCSII.2016.2621120).

[28] P. Deng, *et al.*: "Design of a microstrip low-pass-bandpass diplexer using direct-feed coupled-resonator filter," IEEE Microw. Wireless Compon. Lett. **27** (2017) 254 (DOI: 10.1109/LMWC.2017.2661971).

[29] Y. Liu and K. Chang: "Simple wideband microstrip ring bandpass filter by utilizing forced harmonic suppression and direct feed line coupling," Microw. Opt. Technol. Lett. **54** (2012) 1968 (DOI: 10.1002/mop.26935).

[30] J.-S. Hong and M. J. Lancaster: *Microstrip Filter for RF/Microwave Applications* (Wiley, New York, 2011) 2nd ed.

[31] Q.-X. Chu and H. Wang: "A compact open-loop filter with mixed electric and magnetic coupling," IEEE Trans. Microw. Theory Techn. **56** (2008) 431 (DOI: 10.1109/TMTT.2007.914642).